NASA Technical Memorandum 106012

Interim Report on the Analysis of the Microwave Power Module

Peter Ramins, Raymond W. Palmer,
Dale A. Force, Ben T. Ebihara, Robert P. Gruber, and James A. Dayton, Jr.
Lewis Research Center
Cleveland, Ohio

May 1992

NASA

PRELIMINARY ANALYSIS OF THE MICROWAVE POWER MODULE PERFORMANCE

Peter Ramins, Raymond W. Palmer, Dale A. Force, Ben T. Ebihara, Robert P. Gruber, and James A. Dayton, Jr.

National Aeronautics and Space Administration
Lewis Research Center
Cleveland, Ohio 44135

Summary

The results of a traveling wave tube multistage depressed collector (TWT-MDC) design study in support of the DARPA/DoD Microwave Power Module (MPM) Program are described. The study stressed the MDC as a key element in obtaining the required high overall efficiencies in the MPM application. The results showed that an efficient MDC, utilizing conventional design and fabrication techniques can be designed for the first generation MPM TWT, which permits a package one wavelength thick (.66" at 18 GHz). The overall TWT efficiency goal of 40% for ECM applications appears to be readily achievable. However, the 50% goal for radar applications presents a considerable challenge.

Introduction

This report summarizes the results of the first stage of the NASA-Lewis Traveling Wave Tube-Multistage Depressed Collector (TWT-MDC) design effort in support of the DARPA/Tri-Service Microwave Power Module (MPM) program. The MPM combines a solid state driver, vacuum power booster, and power conditioning in a single module. This first stage of the analysis stressed the MDC as a key element in obtaining the required high overall TWT efficiencies in the MPM application, and addressed the problem of attaining the required high collector efficiency while meeting the stringent system size constraints and practical HV, thermal and mechanical design requirements. The MDC was designed to fit into a first generation MPM (.66" maximum width dimension). The TWT was modelled only at mid-band and its parameters selected to produce a representative spent beam (MDC analysis input) in terms of beam size, space charge, and energy spread. No attempt was made to design and model a broad-band rf (helical) circuit. This approach was based on the observation that, in general, the MDC efficiency is highly insensitive to the operating frequency as such, and an MDC designed for the frequency producing maximum rf output power works well across octave and wider operating bands. The addition of a spent beam refocuser (SBR) with controlled beam expansion, as a key element in obtaining adequately high MDC efficiencies, emerged from the particular combination of size constraints, and cooling and HV stand-off requirements.

Symbols

E_{min} Energy of slowest disk, eV

r_a mean helix radius, inches

$\bar{r}$ average disk radius, inches

V_o Cathode voltage, V

TWT Performance Analysis Results

The TWT performance was analyzed with the Lewis Research Center Helical TWT Computer Code, an extensively revised version of the original Detweiler Program (ref. 1). The input parameters are shown in Table 1(a). In the first stage of this design effort performance analysis was limited to mid-band and the effects of any loading schemes for controlling dispersion were ignored. It is believed that if dispersion effects had been taken into account, similar rf performance and spent beam characteristics would have been obtained with a longer output section. The computed rf performance is summarized in Table 1(b). The spent beam energy distributions at the rf output and after rf debunching are shown in figure 1. The debunching action is almost complete after drift through a tunnel of radius $2r_a$ for

TABLE 1.—INPUT PARAMETERS AND COMPUTED RF PERFORMANCE OF MICROWAVE POWER MODULE TWT OPERATING AT SATURATION AT 12.0 GHz (MIDBAND)

(a) Computer model input parameters

Frequency, GHz	12.0
Average helix radius, in.	0.02
Electron beam radius, in.	0.008
Cathode voltage, kV	3.5
Beam current, mA	175
Center-line interaction impedance, Ω	75
Normalized helix phase velocity, v/c	0.11
Center-line peak magnetic flux density, T	0.3144
Period of PPM magnet stack, in.	0.2169
Length of input helix, in.	0.25
Length of attenuator/sever section, in.	0.50
Length of output helix, in.	1.202
Length of refocuser section, in.	0.271

(b) Computed rf performance

Output power, W	124
Gain, dB	25.7
Input power, dBm	25
RF efficiency, %	20.3
Electronic efficiency, %	22.8
Circuit efficiency, %	89
Circuit losses, W	15.5
Beam interception, W	0

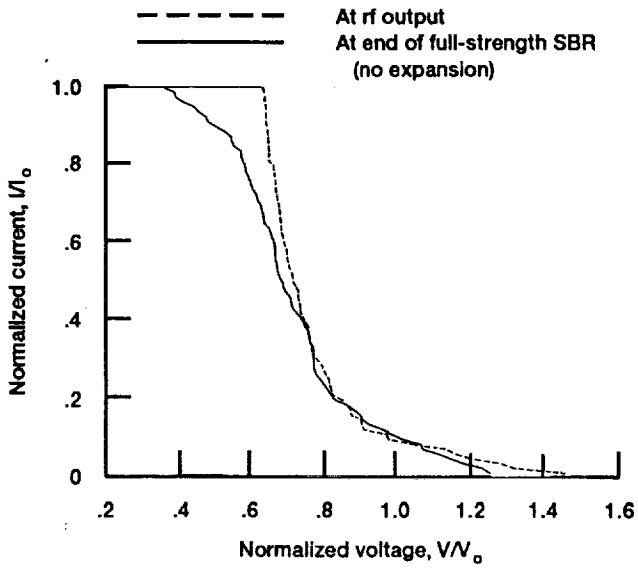

Figure 1.—Computed spent-beam energy at rf output and end of spent beam refocuser with full strength magnets illustrates the effect of debunching. TWT operating at saturation at 12.0 GHz.

1¼ magnetic periods past the rf output (2 magnets), with only small changes in the energy distribution occurring after that. The relatively high values of electronic efficiency of 22.8% and micro perveance of .85 x 10^{-6} $A/V^{3/2}$ combine to produce a surprisingly small velocity spread in the spent beam. However, the effect of debunching is very undesirable with the energy of the slowest electron, E_{min}, being reduced from .64V_o to .36V_o. A part of this reduction in kinetic energy is due to an increase in the space charge potential energy resulting from beam compression as it drifts in a continuation of the PPM stack (from $\bar{r}$ = .58a to $\bar{r}$ = .38a in this case).

Spent Beam Refocuser (SBR) Design and Performance Analysis

The SBR was modelled with the TWT Computer Code so that the effects of beam debunching and controlled expansion could be analyzed simultaneously. It was felt that some controlled beam expansion was mandatory to (1) reduce the amount of kinetic power associated with radial motion resulting from space charge driven beam expansion when the focusing field is removed (power which cannot be recovered in the MDC), and (2) to make possible the design of an MDC sufficiently long so that realistic high-voltage (HV) stand-off and cooling could be provided.

The scope of the SBR investigation, however, was quite limited: (1) only SBR's consisting of 2 or 3 additional magnets of reduced but uniform strength, in a continuation of the PPM stack past the

rf output, were considered, and (2) SBR field strengths in the range of .5 to .7 of nominal were investigated. The SBR design is shown in figure 2; its performance is summarized in Table 2. The .22" long SBR consists of two 60% strength magnets. Compared

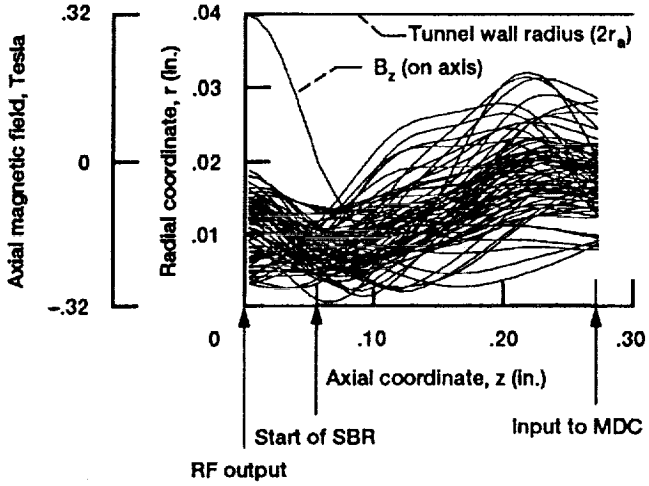

Figure 2.—Disk edge radii trajectories and axial magnetic field in spent beam refocuser (SBR) for TWT operating at saturation at 12.0 GHz. Focusing field in SBR reduced to 60% of TWT magnetic field.

TABLE 2.—SUMMARY OF SPENT BEAM CHARACTERISTICS AT END OF REFOCUSER (INPUT TO MDC)

(a) Range of disk edge angles

Without beam expansion,[a] deg	−17 to +18
With beam expansion,[b] deg	−14 to +5

(b) Average disk edge angle and standard deviation

	Average angle, deg	S_a, deg
Without beam expansion[a]	−1.3	5.5
With beam expansion[b]	−0.5	3.5

(c) Disk edge radii (normalized to drift tunnel radius) and lowest disk energy

	Average radius, $\frac{\bar{r}}{r_a}$	$\frac{r_{max}}{r_a}$ (beam edge)	E_{min}, eV
Without beam expansion[a]	0.19	0.39	1274
With beam expansion[b]	0.43	0.70	1626

[a]Spent beam drifts past rf output in a continuation of the PPM stack with two additional full-strength magnets.

[b]Spent beam drifts past rf output in a continuation of the PPM stack with two additional 60% strength magnets.

to the same beam (at the SBR input) drifting in a full-strength continuation of the PPM stack, it can be seen that the SBR significantly reduces the range and the standard deviation of the disk edge angles at the MDC input, and provides a beam area expansion of more than a factor of five (based on $\bar{r}$). The SBR also provides for conversion of some space charge potential energy into axial kinetic energy. This is illustrated in figure 3. E_{min} is increased from $.36V_o$ to $.46V_o$. The spent beam has an unusually large amount of kinetic energy associated with the fast tail of the distribution (part of which is not recoverable in the MDC). The charge trajectories through the SBR for the unmodulated beam are shown in figure 4.

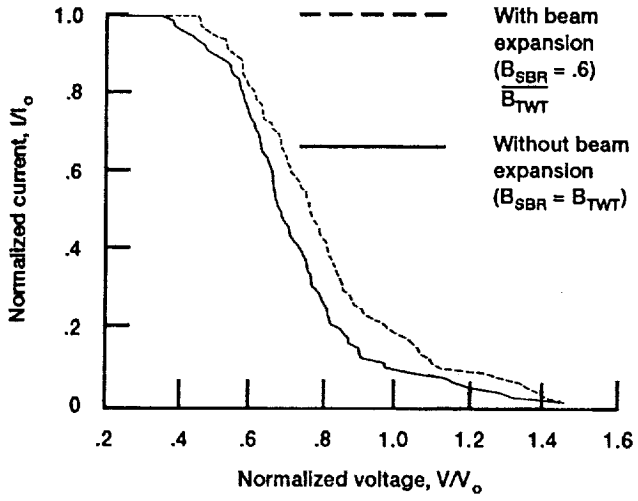

Figure 3.—Computed spent-beam energy at MDC input for TWT operating at saturation at 12.0 GHz illustrates energy recovery in the spent beam refocuser.

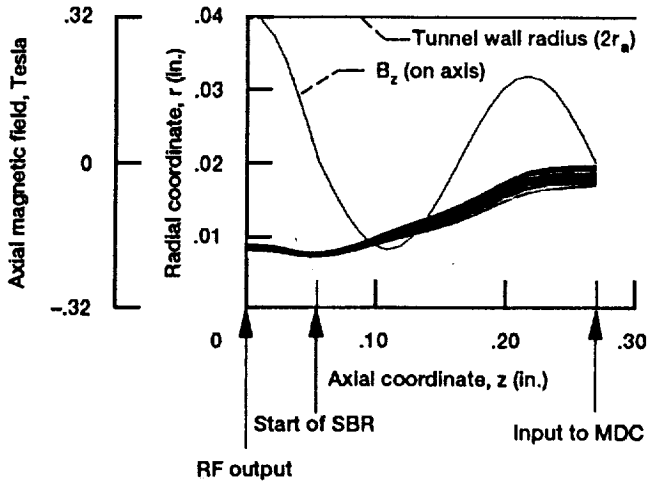

Figure 4.—Disk edge radii trajectories and axial magnetic field in spent beam refocuser (SBR) for TWT operating with "zero" drive power. Focusing field in SBR reduced to 60% of TWT magnetic field.

MDC Design and Performance Analysis

MDC performance was modelled with the Herrmansfeldt Electron Trajectory Computer Program (ref. 2). An MDC active inner diameter of .30" was selected somewhat arbitrarily as a compromise in an attempt to minimize the loss in MDC efficiency that results with decreasing MDC radial size while providing considerable latitude for the HV, thermal, and mechanical designs. Within this size constraint the axial length of the MDC was made as large as possible without significantly compromising the collector efficiency. Both four- and five-stage designs were produced. The four-stage collector design was optimized for operation of the TWT at saturation and does not provide a highly negative ($>.85V_o$) electrode to minimize dissipated power and power density for the zero rf input drive case. The five-stage collector design is a variation of the four-stage design with provision for such an electrode, but it does not represent a fully optimized design for saturated operation of the TWT.

The four-stage, axisymmetric MDC geometry, the applied potentials, the equipotential lines, and the charge trajectories are shown in figures 5 and 6 for the saturated rf and unmodulated (DC) beams, respectively. The corresponding TWT-SBR-MDC power distributions, electrode dissipation, current distributions, and efficiencies are shown in Tables 3 and 4. The overall TWT efficiency includes a heater power of 3W. The corresponding results for the five-stage collector are shown in figures 7 and 8 and Tables 5 and 6. The somewhat low MDC efficiencies of 77.0 to 78.5 percent for the saturated rf cases are due to (1) the large velocity spread in the beam, (2) reduced sorting efficiency (due to the high space charge forces in the spent beam leading to significant irrecoverable energy associated with radial motion (ref. 3)) and (3) the unusually large amount of kinetic power in the high energy tail (ref. 4).

The overall efficiencies are overestimated because the computer model gives zero beam interception. With a more realistic beam interception of 2 percent of the DC beam power, the overall efficiency would be 47.0 and 48.4 percent with the 4 and 5 stage collectors, respectively.

The additional stage (5 versus 4) produces only a modest improvement with the rf beam, but reduces the dissipated power with the unmodulated (DC) beam by almost a factor of two, and the (worst case) thermal power density by more than two. The latter can be seen by comparing the beam impingement areas in figures 6 and 8.

A preliminary look at the HV, mechanical, and thermal designs indicates that it should be possible to incorporate these MDC designs in a practical MPM TWT. However, the packaged MDC could have a considerably larger axial dimension than the .455" active length.

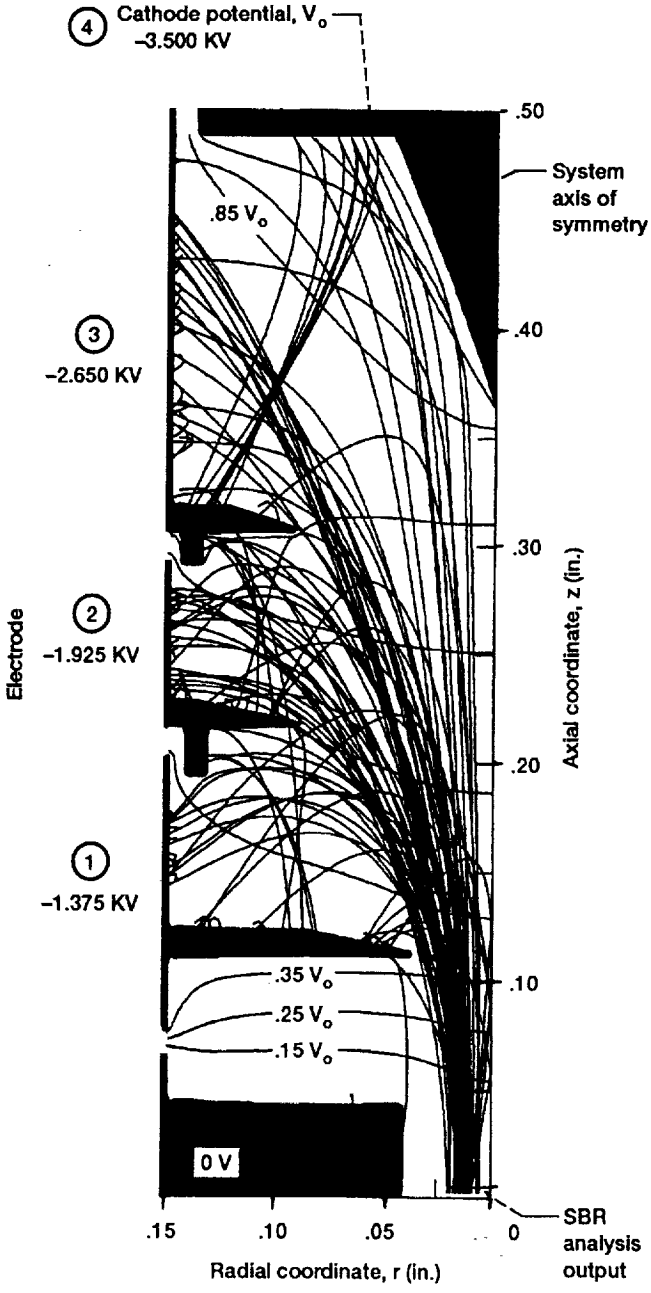

Figure 5.—Charge trajectories in four-stage depressed collector with TWT operating at Saturation at 12.0 GHz. Active MDC size is 0.30" i. d. by 0.455" high.

TABLE 3.—COMPUTED PERFORMANCE OF TWT AND FOUR-STAGE DEPRESSED COLLECTOR, AT SATURATION AT 12.0 GHz

[Computed trajectories shown in fig. 5.]

(a) TWT-SBR-MDC performance[a]

Electrode (fig. 5)	Voltage, kV (with respect to ground)	Current, mA	Recovered power, W	Dissipated power, W
Polepiece	0	1.1	0	1.5
1	−1.375	44.8	61.7	22.4
2	−1.925	63.4	122.1	34.7
3	−2.650	58.0	153.6	33.6
4	−3.500	7.7	26.8	16.9
Totals		175.0	364.2	109.1

(b) Computed efficiency

System component	Efficiency, percent
Collector	77.0
Overall	49.3

(c) Power balance in TWT-SBR-MDC system

Component of power	Power, W
Beam interception	0
Total RF conversion	[b]139.6
Recovered power	364.2
MDC dissipation	109.1
Total	612.9

[a]Assumes an (isotropic-graphite) electrode secondary-electron-emission yield of 0.5.

[b]Includes output power of 124.1 w, window losses of 0 w, and circuit losses of 15.5 w.

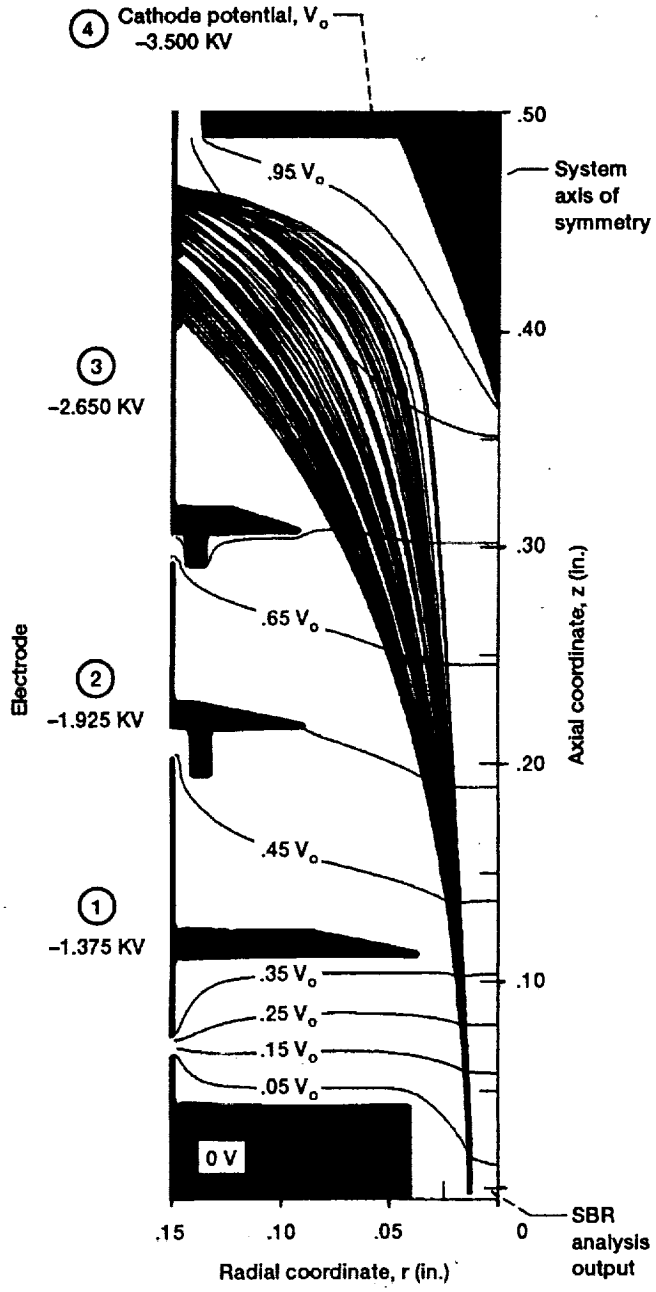

Figure 6.—Charge trajectories in four-stage depressed collector with unmodulated (DC) beam. Active MDC size is 0.30" i. d. by 0.455" high.

TABLE 4.—COMPUTED PERFORMANCE OF TWT AND FOUR-STAGE DEPRESSED COLLECTOR WITH UNMODULATED (DC) BEAM

[Computed trajectories shown in fig. 6.]

(a) TWT-SBR-MDC performance[a]

Electrode (fig. 6)	Voltage, kV (with respect to ground)	Current, mA	Recovered power, W	Dissipated power, W
Polepiece	0	0	0	0
1	−1.375	0	0	0
2	−1.925	0	0	0
3	−2.650	175.0	463.7	149.2
4	−3.500	0	0	0
Totals		175.0	463.7	149.2

(b) Computed efficiency

System component	Efficiency, percent
Collector	75.7
Overall	0

(c) Power balance in TWT-SBR-MDC system

Component of power	Power, W
Beam interception	0
Total RF conversion	0
Recovered power	463.7
MDC dissipation	149.2
Total	613.3

[a]Assumes an (isotropic-graphite) electrode secondary-electron-emission yield of 0.5.

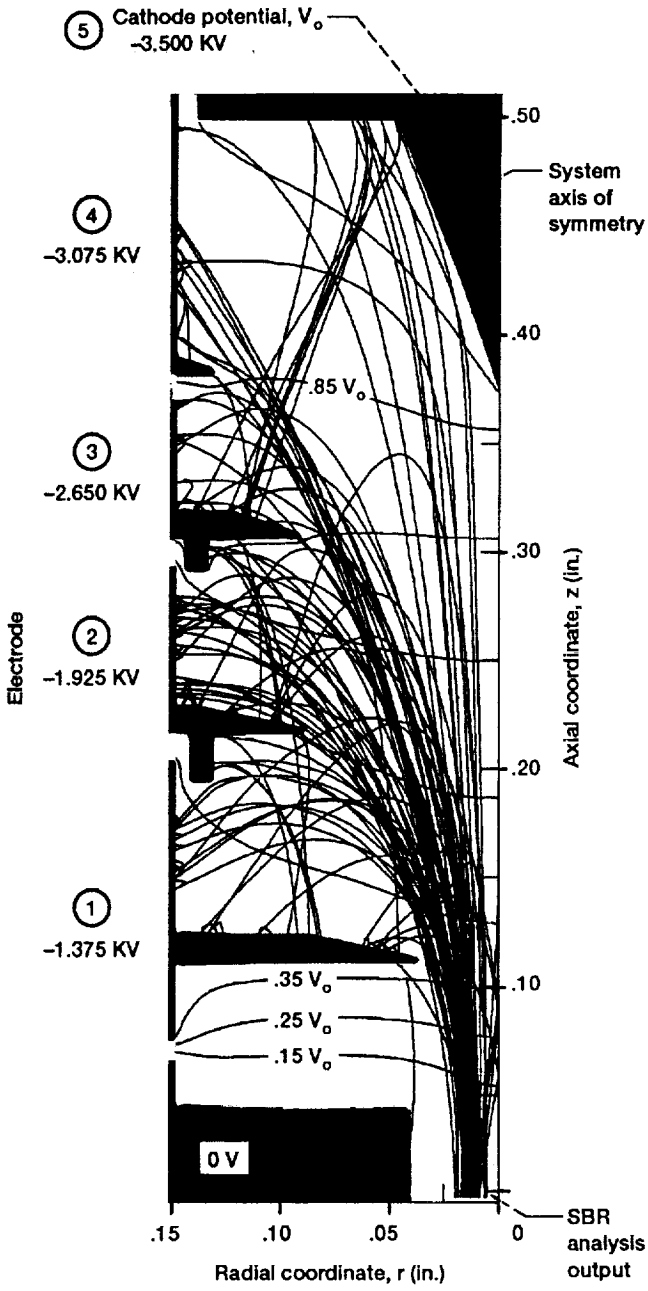

Figure 7.—Charge trajectories in five-stage depressed collector with TWT operating at saturation at 12.0 GHz. Active MDC size is 0.30" i. d. by 0.455" high.

TABLE 5.—COMPUTED PERFORMANCE OF TWT AND FIVE-STAGE DEPRESSED COLLECTOR, AT SATURATION AT 12.0 GHz

[Computed trajectories shown in fig. 7.]

(a) TWT-SBR-MDC performance[a]

Electrode (fig. 7)	Voltage, kV (with respect to ground)	Current, mA	Recovered power, W	Dissipated power, W
Polepiece	0	1.1	0	1.5
1	-1.375	44.8	61.7	22.4
2	-1.925	65.6	126.3	37.3
3	-2.650	35.0	92.8	14.3
4	-3.075	20.8	63.9	9.4
5	-3.500	7.7	26.8	16.9
Totals		175.0	371.4	101.9

(b) Computed efficiency

System component	Efficiency, percent
Collector	78.5
Overall	50.8

(c) Power balance in TWT-SBR-MDC system

Component of power	Power, W
Beam interception	0
Total RF conversion	[b]139.6
Recovered power	371.4
MDC dissipation	101.9
Total	612.9

[a]Assumes an (isotropic-graphite) electrode secondary-electron-emission yield of 0.5.

[b]Includes output power of 124.1 w, window losses of 0 w, and circuit losses of 15.5 w.

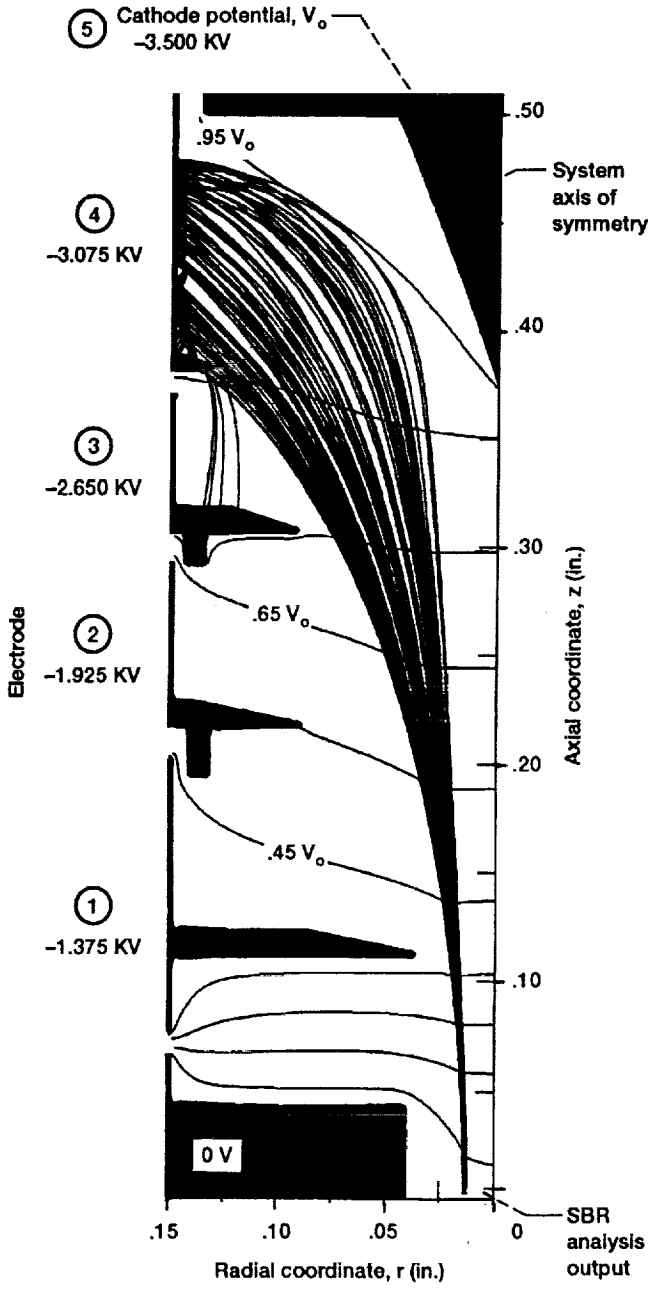

Figure 8.—Charge trajectories in five-stage depressed collector with unmodulated (DC) beam. Active MDC size is 0.30" I. d. by 0.455" high.

TABLE 6.—COMPUTED PERFORMANCE OF TWT AND FIVE-STAGE DEPRESSED COLLECTOR WITH UNMODULATED (DC) BEAM

[Computed trajectories shown in fig. 8.]

(a) TWT-SBR-MDC performance[a]

Electrode (fig. 8)	Voltage, kV (with respect to ground)	Current, mA	Recovered power, W	Dissipated power, W
Polepiece	0	0	0	0
1	−1.375	0	0	0
2	−1.925	0	0	0
3	−2.650	5.5	14.5	2.3
4	−3.075	169.5	521.3	74.8
5	−3.500	0	0	0
Totals		175.0	535.8	77.1

(b) Computed efficiency

System component	Efficiency, percent
Collector	87.4
Overall	0

(c) Power balance in TWT-SBR-MDC system

Component of power	Power, W
Beam interception	0
Total RF conversion	0
Recovered power	535.8
MDC dissipation	77.1
Total	613.3

[a]Assumes an (isotropic-graphite) electrode secondary-electron-emission yield of 0.5.

A summary of the estimated MPM performance is presented in Table 7. A somewhat conservative value of electronic power conditioner (EPC) efficiency of 84 percent was assumed.

TABLE 7.—SUMMARY OF NASA ESTIMATES OF MICROWAVE POWER MODULE SYSTEM PERFORMANCE FOR TWT WITH FIVE-STAGE DEPRESSED COLLECTOR

	Untapered helix	
	Saturation at 12.0 GHz	DC
Beam voltage, kV	3.5	3.5
Beam current, mA	175	175
RF output at 12 GHz, W	124	0
RF losses, W	16	0
Beam interception, W	12	6
Heater power, W	3	3
Collector dissipation, W	102	77
SS driver input, W	11	10
EPC losses, W	50	20
TWT efficiency, percent	48.4	0
MPM efficiency, percent	39.1	0
Total dissipation, W	193	116
Total power, W	317	116

Concluding Remarks

This initial design study was aimed at a first generation MPM which permits a .66" width. The results showed that an efficient MDC, utilizing conventional HV stand-off, thermal, and mechanical design and fabrication techniques, can be designed for the MPM TWT. The overall TWT efficiency goal of 40% for electronic counter measure (ECM) applications appears to be readily achievable. However, the 50% goal for radar applications presents a considerable challenge. A preliminary look at MDC fabrication and possible electronic power conditioning (EPC) approaches indicates that the fairly large number of collector stages considered in this study (4 and 5) does not represent a significant complication. The improved efficiency, compared to 2 and 3 stages, leads to substantially lower prime power and simplifies the cooling problem.

The second stage of the NASA-Lewis design study will (1) take a closer look at higher electronic efficiency broad-band helical circuits with reduced beam current and space charge, (2) extend the TWT-MDC performance analysis to band-edges, and (3) investigate smaller MDC's for the next generation of MPM TWT's.

References

1. Detweiler, H.K.: Characteristics of Magnetically Focused Large Signal Traveling-Wave Amplifiers. Ph.D. Thesis. University of Michigan, Ann Arbor, MI, 1968.

2. Herrmannsfeldt, W.B.: Electron Trajectory Program—SLAC Computer Program. Report SLAC-226. Standford Linear Accelerator Center, CA, 1979.

3. Kosmahl, H.G.: Modern Multistage Depressed Collectors—A Review. Proc. IEEE, vol. 70, Nov. 1982, pp. 1325-1334.

4. Kosmahl, H.G.: How to Quickly Predict the Overall TWT and the Multistage Depressed Collector Efficiency. IEEE Trans. Electron Devices, vol. ED-27, Mar. 1980, pp. 526-529.

REPORT DOCUMENTATION PAGE

Form Approved
OMB No. 0704-0188

1. AGENCY USE ONLY (*Leave blank*)	2. REPORT DATE	3. REPORT TYPE AND DATES COVERED
	May 1992	Technical Memorandum

4. TITLE AND SUBTITLE

Interim Report on the Analysis of the Microwave Power Module

5. FUNDING NUMBERS

WU-506-72

6. AUTHOR(S)

Peter Ramins, Raymond W. Palmer,
Dale A. Force, Ben T. Ebihara, Robert P. Gruber, and James A. Dayton, Jr.

7. PERFORMING ORGANIZATION NAME(S) AND ADDRESS(ES)

National Aeronautics and Space Administration
Lewis Research Center
Cleveland, Ohio 44135-3191

8. PERFORMING ORGANIZATION REPORT NUMBER

E-7384

9. SPONSORING/MONITORING AGENCY NAMES(S) AND ADDRESS(ES)

National Aeronautics and Space Administration
Washington, D.C. 20546-0001

10. SPONSORING/MONITORING AGENCY REPORT NUMBER

NASA TM-106012

11. SUPPLEMENTARY NOTES

Responsible person, Peter Ramins, (216) 433-3521.

12a. DISTRIBUTION/AVAILABILITY STATEMENT

Unclassified - Unlimited
Subject Category 33

12b. DISTRIBUTION CODE

13. ABSTRACT (*Maximum 200 words*)

The results of a traveling wave tube multistage depressed collector (TWT-MDC) design study in support of the DARPA/DoD Microwave Power Module (MPM) Program are described. The study stressed the MDC as a key element in obtaining the required high overall efficiencies in the MPM application. The results showed that an efficient MDC, utilizing conventional design and fabrication techniques can be designed for the first generation MPM TWT, which permits a package one wavelength thick (.66" at 18 GHz). The overall TWT efficiency goal of 40% for ECM applications appears to be readily achievable. However, the 50% goal for radar applications presents a considerable challenge.

14. SUBJECT TERMS

Traveling wave tube multistage; Depressed collector high efficiency

15. NUMBER OF PAGES

14

16. PRICE CODE

A03

17. SECURITY CLASSIFICATION OF REPORT	18. SECURITY CLASSIFICATION OF THIS PAGE	19. SECURITY CLASSIFICATION OF ABSTRACT	20. LIMITATION OF ABSTRACT
Unclassified	Unclassified	Unclassified	